Anomalous Diffusion and Oscillations in an Afterglow Plasma

T. Dodo[+)]

IPP 2/65 November 1967

INSTITUT FÜR PLASMAPHYSIK

GARCHING BEI MÜNCHEN

INSTITUT FÜR PLASMAPHYSIK

GARCHING BEI MÜNCHEN

Anomalous Diffusion and Oscillations in an Afterglow Plasma

T. Dodo[+)]

IPP 2/65 November 1967

+) Guest from the Central Research Laboratory, Hitachi Ltd., Kokubunji, Tokio/Japan.

Die nachstehende Arbeit wurde im Rahmen des Vertrages zwischen dem Institut für Plasmaphysik GmbH und der Europäischen Atomgemeinschaft über die Zusammenarbeit auf dem Gebiete der Plasmaphysik durchgeführt.

IPP 2/65 T. Dodo Anomalous Diffusion and Oscillations in an Afterglow Plasma

in English (November 1967)

Abstract

Diffusion and oscillations of helium and neon plasmas have been examined in a glass chamber. The method of the experiment is the same as in the experiment in a metal chamber [1].

The diffusion coefficient and the behavior of the oscillations in the plasma is quite the same as in the case of metal chamber. When $\omega_{ci}\tau_{in} < 1$, there are no oscillations in the plasma density, and the diffusion is classical. When $\omega\tau > 1$, oscillations appear in the plasma density and the diffusion becomes anomalous and o.3 times Bohm diffusion.

The shape of the fluctuation of the plasma potential is the same over the plasma volume and the fluctuating electric field is very small (< 0.2 mV/cm), when $\omega\tau < 1$. When $\omega\tau > 1$, the fluctuation of the plasma potential becomes turbulent and the amplitude of fluctuating electric field becomes large ($\gtrsim 3$ mV/cm).

I. Introduction

Usually, the diffusion of a plasma in a glass chamber differs from that in a metal chamber. In the experiment of Geissler [2, 3], the diffusion is anomalous and of Bohm-type in the case of a metal chamber, whereas it is classical in the case of a glass chamber. In his method of experiment, the usual method of decay time measurement of an afterglow plasma, the electrons arrive at the axial wall and the ions arrive at the radial wall and both recombine on the metal wall. On the other hand, in the spread-out time measurement [1] the plasma has not yet arrived at the radial wall. Therefore, the influence of the chamber wall to the plasma diffusion in the decay time measurement must be different from that in the spread-out time measurement. The axial diffusion is only a small correction for obtaining the diffusion coefficient across the magnetic field from the spread-out time. The radial wall must have no influence on the spread-out time. For this reason, it is expected that in the present experiment the diffusion coefficient across the magnetic field in a glass chamber is similar to that in a metal chamber. This supposition is examined by doing an experiment with a glass chamber inserted into a metal chamber.

II. Experimental Apparatus

A glass cylinder of 17 cm inner diameter and 70 cm long is inserted into a metal vacuum chamber (Fig. 1). The magnetic field is uniform within $\pm$ 1 % inside the glass chamber.

The method of the plasma production and the vacuum condition is the same as reported earlier [1]. The plasma is produced by an electron beam pulse with acceleration voltage of 400 V, beam current of 0.1 ~ 0.5 mA, and 1 msec pulse width. The base pressure is 3×10^{-8} torr; spectroscopically

pure helium flows continuously through the system at a pressure of 20 to 100 m torr.

The ion density is measured by a circular Langmuir probe of 4 mm in diameter, which is biased to -2.7 volt with respect to the grounded metal chamber.

A fork-type probe shown in Fig. 2 lies in a plane perpendicular to the magnetic field. A Langmuir probe is inserted into the same plane, azimuthally displaced from the fork-type probe by 90°. This fork probe is movable in the radial direction and can be rotated around its axis. When this probe is horizontal (the B-field is vertical), it picks up the fluctuating electric field in θ-direction. When it is placed in vertical position, it picks up the fluctuating electric field in z-direction. This probe is either held approximately at plasma potential, or floated over a 100 pF capacitor.

III. Experimental Results

Plasma Potential

The floating potential of the plasma is measured by the Langmuir probe which is in series with a 100 MΩ resistor. Some examples are shown in Fig. 3. Because the electron temperature is very low (300 $^{\circ}$K), the plasma potential is nearly equal to the floating potential. The plasma potential is a function of position, magnetic field strength, time after the ionizing pulse, and is usually from -0.2 to -0.8 volt with regard to the ground potential. (The anode of the electron gun and the metal vacuum chamber are grounded). In the case of the metal chamber, the plasma potential, which was +0.3 ~ +0.5 V with respect to ground potential, was not strongly dependent on the magnetic field strength and was

rather uniform in space. In the case of the glass chamber, the plasma potential is strongly dependent on the magnetic field strength as seen in Fig. 3 and the potential distribution is not uniform in space (Fig. 3A). Because the time constant of the measuring circuit is large (> 10 msec), the fluctuation of the plasma potential cannot be observed by this method. For the measurement of the fluctuating plasma potential, the probe is connected to the oscilloscope through a 100 pF capacitor.

The Dependence of the Diffusion Coefficient on the Magnetic Field Strength

The diffusion coefficient is measured by the spread-out time of the plasma as explained in [1]. The ion saturation current into the Langmuir probe, which is located off the central axis of the chamber, is very small at first and reaches maximum as the plasma diffuses outwards, and then decreases as the plasma decays. The time τ_s at which the ion current becomes maximum is related to the diffusion coefficient $D_\perp$ in the formula $\tau_s = r^2/4D_\perp$, where r is the distance between the probe and the axis. The dependence of the diffusion coefficient on the magnetic field strength is quite similar to the case of the metal chamber. When $\omega_{ci}\tau_{in} < 1$, where ω_{ci} is the ion cyclotron frequency and τ_{in} is the collision time between the ions and neutral atoms, the spread-out signal is very smooth and agrees well with the theoretical prediction (Fig. 4). The dependence of the spread-out time τ_s on the magnetic field strength is proportional to the square of the magnetic field (Fig. 5). The experimental data for various gas pressures can be expressed in a simplified way when τ_s/p is expressed as a function of B/p. The experimental points lie on a single curve and those fit well with the classical ambipolar diffusion (Fig. 6), but the theoretical values of the classical ambipolar diffusion $(\tau_s/p)_{amb}$ are reduced by a factor of 9.

$$(\tau_s/p)_{amb} = r^2/D_\perp p = (r^2/4D_\parallel p)(1 + \omega_{ci}\tau_{in}\omega_{ce}\tau_{en}).$$

In the case of the metal chamber, $(\tau_s/p)_{exp}$ was one-tenth of $(\tau_s/p)_{amb}$. The absolute values of diffusion coefficient in the glass chamber are quite similar to the values in the metal chamber, and the dependence of the diffusion coefficient on the magnetic field strength in both cases agrees with the classical diffusion.

When $\omega_{ci}\tau_{in} > 1$, irregular oscillations appear in the probe signal (Fig. 7). The spread-out time over neutral gas pressure τ_s/p is proportional to B/p instead of $(B/p)^2$ (Fig. 8). The numerical value is

$$(\tau_s/p)_{exp} = \frac{0.9}{4\times10^4}\ \frac{B}{p}\ .$$

From the relation $D_\perp = r^2/4\tau_s$, the diffusion coefficient is

$$(D_\perp)_{exp} = 4.4 \times 10^4\ \frac{1}{B} \simeq 0.3 \times \frac{1}{16}\ \frac{ckT}{eB}\ (T = 300\ ^\circ K),$$

i.e. the diffusion coefficient is about one-third of the Bohm diffusion coefficient. In the case of the metal chamber, the diffusion coefficient was about 0.4 times Bohm diffusion.

Diffusion in Neon Gas

The plasma potential in neon gas plasma is mainly positive (Fig. 9). Similarly to the case of helium gas, in the case of neon gas the spread-out signal is very smooth when $\omega\tau < 1$ (Fig. 10). In neon gas, the critical magnetic field for the anomalous diffusion and the appearance of the oscillation is much higher than that in helium gas, because $(\omega\tau)_{Ne}$ is 3.2×10^{-5} (B/p) and $(\omega\tau)_{He}$ is 8.3×10^{-5}(B/p).

When $\omega\tau > 1$, the oscillation appears in the spread-out signal (Fig. 11).

The Spread-out Time of Electrons

When the Langmuir probe is positively biased, one observes electron current to the probe. In this case the result is very similar to the case of the ion diffusion. When $\omega_{ci}\tau_{in} < 1$, the spread-out signal of electrons has regular form (Fig. 12). When $\omega_{ci}\tau_{in} > 1$, the spread-out signal contains oscillation (Fig. 13). However, the frequency of the oscillation is much higher than the case of the ion current. When a part of the spread-out signal is displayed with a faster time sweep, one can observe the frequency of this oscillation (~ 2 kc)(Fig. 13A). The dependence of the diffusion coefficient on the magnetic field strength in the case $\omega\tau > 1$ is also Bohm-type (Fig. 14). The numerical values are very near to the values in the case of the ion current.

Oscillations in the Plasma

Two Langmuir probes are inserted into the chamber in a plane perpendicular to the magnetic field and 90 degrees apart. Each probe signal is introduced to a dual-beam oscilloscope through a 100 pF capacitor. In this measurement, oscillations can be observed even when $\omega\tau < 1$. When $\omega\tau > 1$, the amplitude of this oscillation becomes a little larger and its frequency becomes lower. An example is shown in Fig.15 when $\omega\tau < 1$. Oscillations appearing in these two probes are completely the same. The input impedance of both probes are exactly the same. Using a faster time sweep, it is still difficult to observe the time lag between the signals (Fig. 16). In the case of Fig. 16, the time lag is shorter than

10 μsec and the distance between the probes is 5.7 cm, and the phase velocity in θ - direction is larger than 5.7 cm/10 μsec $\simeq$ 6 x 10^5 cm/sec. This phase velocity is faster than the ion thermal velocity ~1 x 10^5 cm/sec.

When the magnetic field strength is large and $\omega\tau$ is larger than about 3, the oscillation amplitude becomes a little larger, but it is still smaller than thermal energy of the plasma. The oscillation frequency becomes lower and the oscillations in both probes are quite different in form (Fig. 17).

The fluctuating electric field in the plasma is measured by a fork probe. Each branch of the fork probe is inserted into one of the two inputs of the oscilloscope, and the difference of the floating potentials is measured. The plasma potential is very near to the floating potential; therefore the output of the differential amplifier displays the fluctuating electric field. When $\omega\tau > 1$, the oscillation of the fluctuating electric field is different from the oscillation of the density fluctuation measured by the biased Langmuir probe (Fig. 7).

When the fork probe is in a plane perpendicular to the magnetic field, the amplitude of the oscillation is large (Fig. 18). When the fork probe is in a plane parallel to the magnetic field, the amplitude of oscillation is small (Fig. 19), i.e. the fluctuating electric field is mainly in the ϑ- direction.

The amplitude of the fluctuating electric field is extremely small when $\omega\tau < 1$ (Fig. 20). On the other hand, the amplitude of the fluctuating plasma potential is not so small even when $\omega\tau$ is smaller than 1 (Fig. 21). The ratio of the amplitude of the fluctuating electric field at $\omega\tau = 5$ to that at $\omega\tau = 0.8$ is much larger than the ratio of the amplitude of the fluctuating plasma potential at $\omega\tau = 5$ to that at $\omega\tau = 0.8$ (Figs. 20, 21). When $\omega\tau < 1$, the oscillation of the plasma potential is uniform in space (Figs. 15, 16).

Therefore, the fluctuating electric field, the difference of the plasma potential in different position , is extremely small. When $\omega\tau > 1$, the oscillation of the plasma potential becomes turbulent in space. Therefore, the fluctuating electric field becomes large.

Oscillations appearing in each branch of the fork probe are also observed separately. When the fork probe is in the plane perpendicular to the magnetic field, the oscillations have different forms (Fig. 22). Therefore, the fluctuating electric field, which is the difference between these signals, is large in this plane. When the fork probe is in a plane parallel to the magnetic field, the oscillations have nearly the same form (Fig. 23) and the difference between the oscillations, the electric field, is small.

In the z-direction, however, the wave length of the fluctuating plasma potential is very large.The oscillations in the metal chamber are quite similar to the oscillations in the glass chamber. An additional measurement was possible in the metal chamber: another Langmuir probe was inserted at the end of the uniform magnetic field. The distance between the probe in the midplane and the end probe is 35 cm. The floating potentials appearing in these two probes are displayed on a dual-beam oscilloscope (Fig. 24). The phase difference is about $\pi/2$, i.e. in the tube length (70 cm) there is a half wave length. The phase velocity in z-direction is about $35\text{cm}/80\,\mu\text{sec} \simeq 4 \times 10^5$ cm/sec.

The frequency spectrum is measured by a spectrum analyser. The Langmuir probe is connected to a spectrum analyser through a 100 pF capacitor. When $\omega\tau \lesssim 1$, the frequency is about 2 kc (Fig. 25). When the magnetic field is stronger, the frequency becomes lower (Fig. 26) and lower (Fig. 27). However, it is difficult to get a quantative functional relation between the oscillation frequency and the magnetic field strength or $\omega\tau$.

Discussion

The diffusion of the afterglow plasma in a glass chamber seems to be the same mechanism as that in a metal chamber. Therefore, in this afterglow plasma the short circuit effect proposed by Simon [4] is not applicable.

When $\omega\tau < 1$, there is no oscillation in the spread-out signal and the diffusion is classical. There is a small amplitude oscillation in the plasma potential. The oscillations appearing in two Langmuir probes, which are separated by 90 degrees, are completely the same. The amplitude of the fluctuating electric field is negligible small.

When $\omega\tau < 1$, the dependence of the diffusion coefficient on the magnetic field strength is classical, but the absolute value is 9 times as large as the classical value. One may attribute this factor to the effect of electron temperature. However, if one wants to explain this factor by the higher collision frequency of the electrons, one must assume the electron temperature as about 2700 ^{o}K. This temperature is too high for the electron temperature of an afterglow plasma. The numerical value of the classical diffusion coefficient in the present experiment is still open to question.

When $\omega\tau > 1$, oscillations appear in the spread-out signal and the diffusion becomes anomalous and Bohm-type. The oscillation amplitude in the plasma potential becomes large. The oscillation in a probe is quite different from that in the other probe. The amplitude of the fluctuating electric field is very large. The oscillation in the plasma becomes turbulent. The regular oscillation of the plasma potential in the case $\omega\tau < 1$ does not affect the diffusion. The turbulent oscillation of the fluctuating electric field enhances the plasma diffusion anomalously.

The present experimental results contradict Geissler's results [2]. Recently, Geissler [5] reported that when the

end plate of the metal chamber is electrically floated against the side wall, the diffusion becomes classical ambipolar diffusion and that the loss of high energy tail of the Maxwellian distribution of electrons plays an important role in the anomalous diffusion of the afterglow plasma. In the present experiment, however, the diffusion in a glass chamber is still anomalous when $\omega\tau$ is larger than 1.

In a metal chamber, Geissler obtained 2.2 times Bohm diffusion, whereas the anomalous diffusion in the present method is 0.4 times Bohm diffusion. In the present experiment, sometimes the oscillation amplitude grows in the later parts of the decay (Fig. 28). The usual decay time measurement is carried out in the later period of the decay, whereas the present method is concerned with the earlier spread-out period where the oscillation amplitude is smaller. Therefore, the present method yields a smaller diffusion coefficient.

The density gradient of the plasma is steeper in the period of spread-out than the decay period. Nevertheless the oscillation amplitude is sometimes larger in the decay period. Also the oscillation frequency is not strongly dependent on the magnetic field strength. Therefore, these oscillations are most likely not drift waves ($\frac{\omega}{k} \sim \frac{T}{B} \frac{\nabla n}{n}$).

Zhilinsky et.al. [6] obtained an interesting result in a decay time measurement in a glass chamber. They demonstrated that when the tube radius of the chamber becomes larger, the diffusion coefficient becomes smaller and approaches the classical value. This result indicates that the plasma becomes stable against the drift instability when $\nabla n/n$ is not too large. In the present experiment, the probe's radial position corresponds roughly to Zhilinsky's tube radius. However, here, even when the probe is 6 cm off the central axis, oscillations are observed in the spread-out

signal when $\omega\tau$ is larger than 1.

Golant [7] pointed out that the potential difference between the biased Langmuir probe and the grounded metal chamber will cause a $E_r \times B_z$ drift. (In the present experiment there is a metal chamber for the purpose of the vacuum chamber outside the glass cylinder). This drift will enhance the drift instability. In the present experiment, positive or negative potential is applied to a probe and the fluctuation in the plasma potential is measured by the other probe. The oscillation amplitude becomes a little ($\sim$ 1.5 times) larger when the bias potential is applied to the first probe. However, the frequency spectrum in the second probe does not change when the potential is applied to the first probe. This implies that the potential applied to the probe has no essential effect on the instability in the present experiment.

In concluding, it should be emphasized that the anomalous diffusion is closely correlated to the turbulent fluctuation of the electric field in the plasma [8]. When $\omega\tau > 1$, the turbulent oscillation of the fluctuating electric field appears and the diffusion becomes anomalous.

The author thanks heartily Drs. von Gierke, Blau, Grieger, Tasso, Golant, and Zhilinsky for their helpful advices and interesting discussions.

References

[1] T. Dodo, IPP 2/62, Munich (1967)

[2] K.H. Geissler, IPP 2/50, Munich (1966)

[3] K.H. Geissler, IPP 2/51, Munich (1966)

[4] A. Simon, Phys.Rev. 98, 317 (1955)

[5] K.H. Geissler, Paper presented at "Symposium on fluctuations and diffusion in plasmas", Princeton, 1967

[6] A.P. Zhilinsky et.al., 8th Int.Conf.on Phenomena on Ionized Gas, Vienna,p.318, 1967

[7] V.E. Golant, Private communication

[8] L. Spitzer, Phys.Fluids 3, 659 (1960)

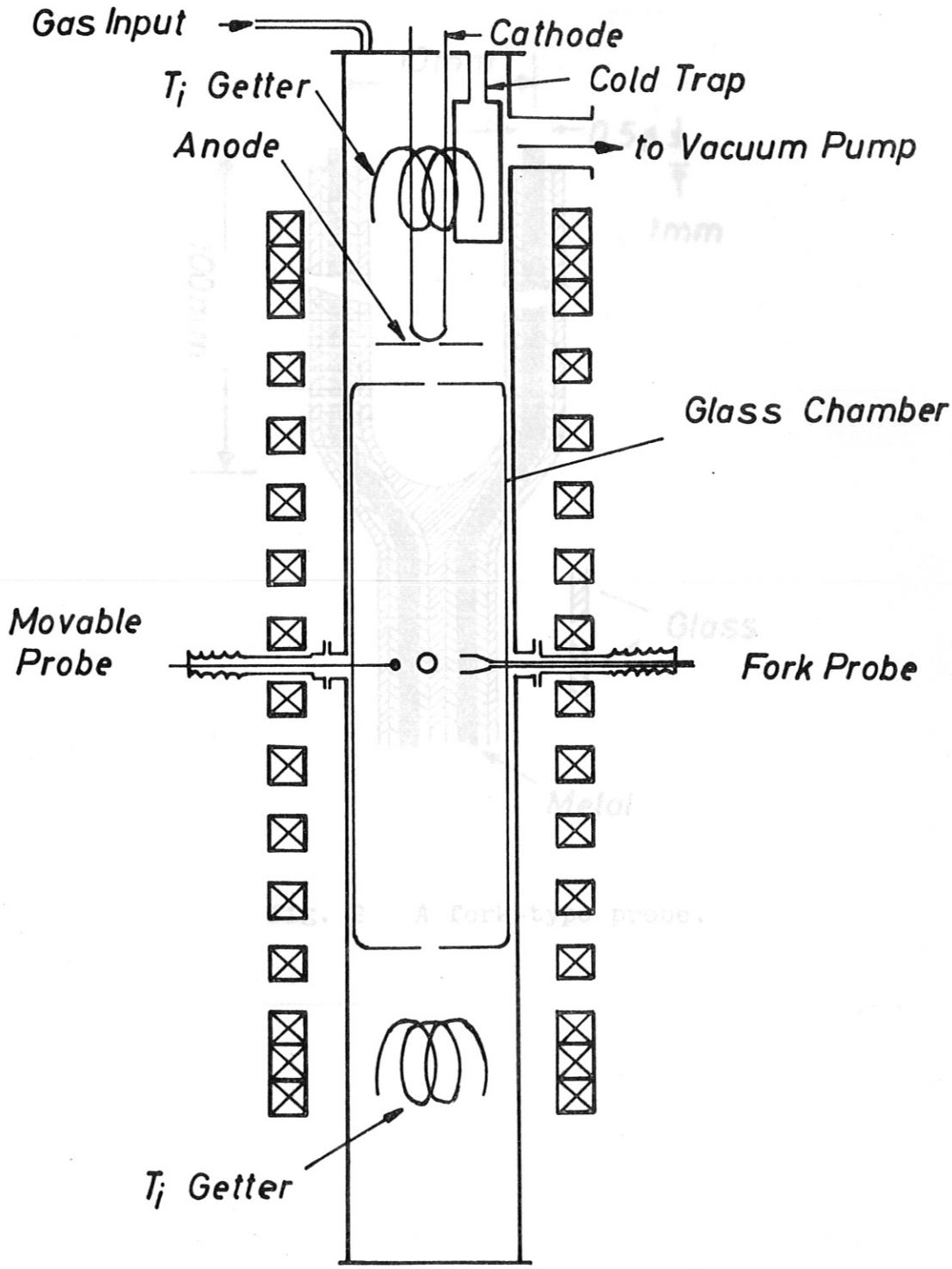

Fig. 1 Schematic drawing of the experimental apparatus.

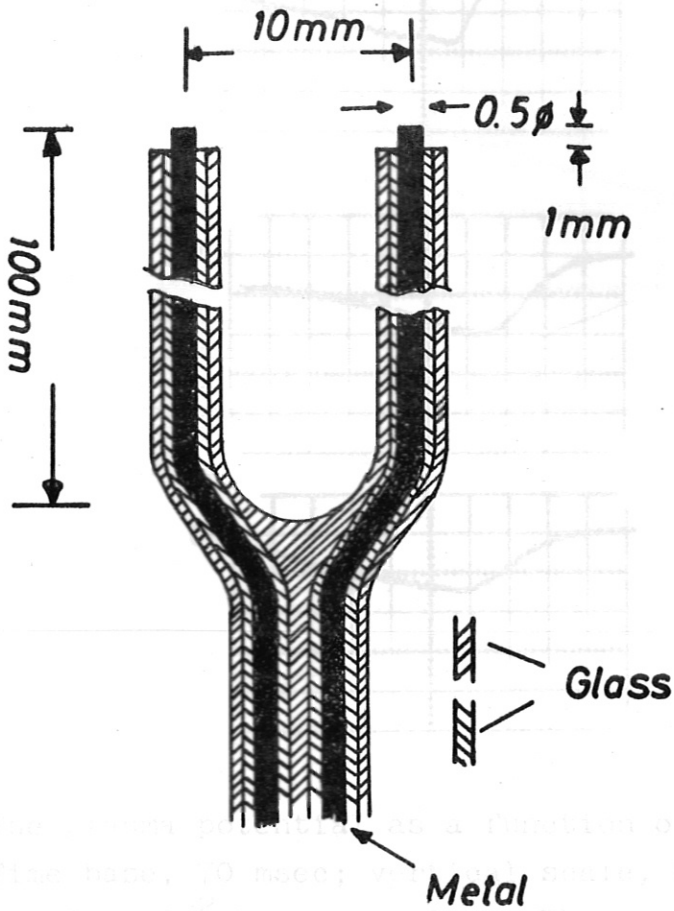

Fig. 2 A fork-type probe.

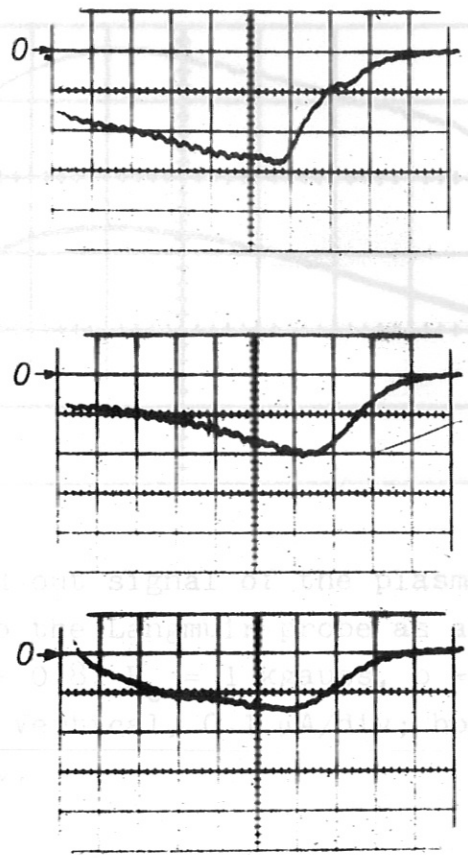

Fig. 3 The plasma potential as a function of time. Time base, 70 msec; vertical scale, 0.2 /div; $p = 5 \times 10^{-2}$ torr; r = 2 cm. The magnetic field strength is 0.5, 1.5, and 3 kgauss, respectively.

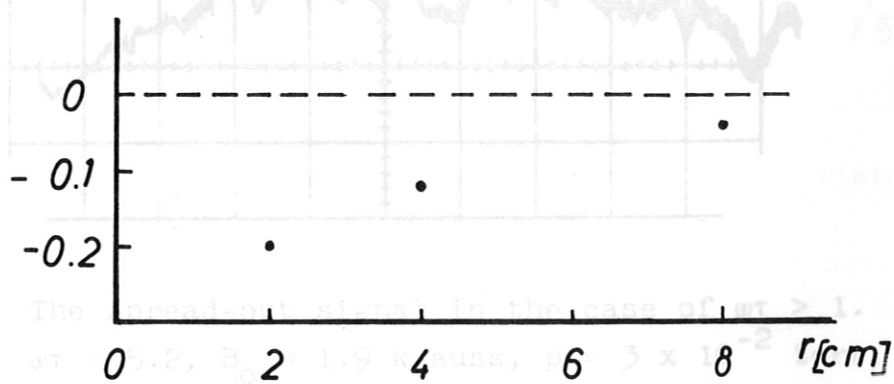

Fig. 3A The plasma potential as a function of position. $\omega\tau = 2.5$, $B_o = 1.5$ kgauss, $p = 5 \times 10^{-2}$ torr, 100 msec after the ionizing pulse.

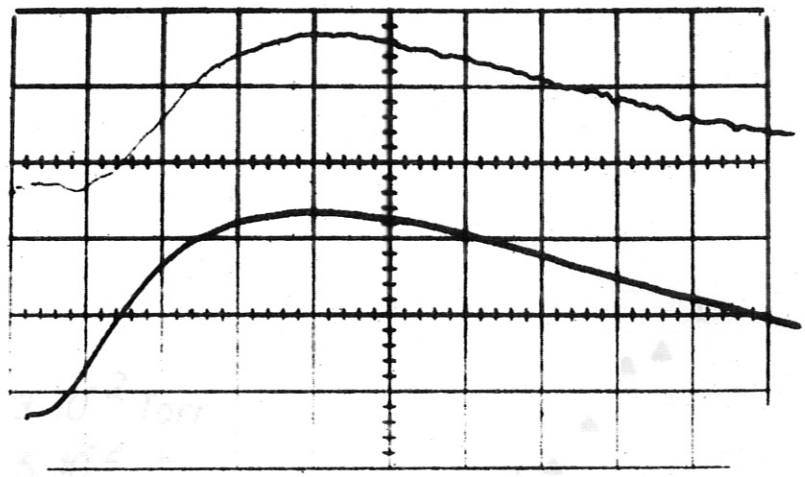

Fig. 4 The spread-out signal of the plasma, the ion current to the Langmuir probe as a function of time. $\omega\tau = 0.8$, $B_o = 1$ kgauss, $p = 1 \times 10^{-1}$ torr, $r = 2$ cm. Vertical, 0.1 μA/div; horizontal, 5 msec/div.

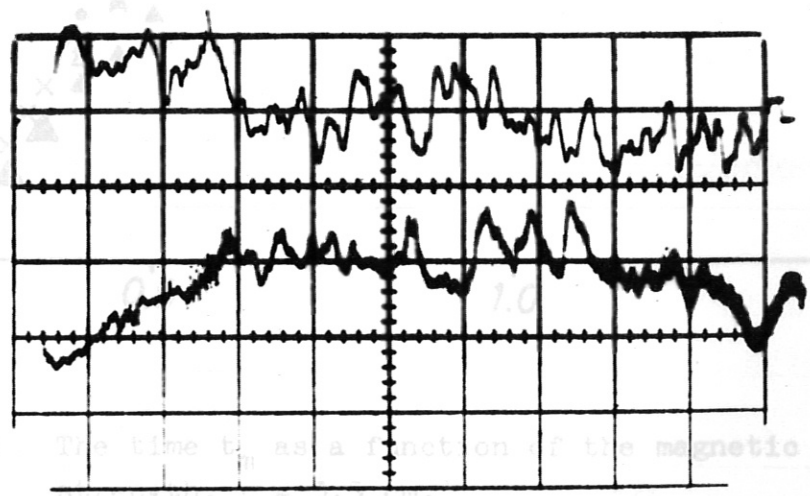

Fig. 7 The spread-out signal in the case of $\omega\tau > 1$. $\omega\tau = 5.2$, $B_o = 1.9$ kgauss, $p = 3 \times 10^{-2}$ torr, $r = 2$ cm. Vertical, 0.03 μA/div; horizontal, 5 msec/div. Upper trace: fork probe signal, 10 mV/div.

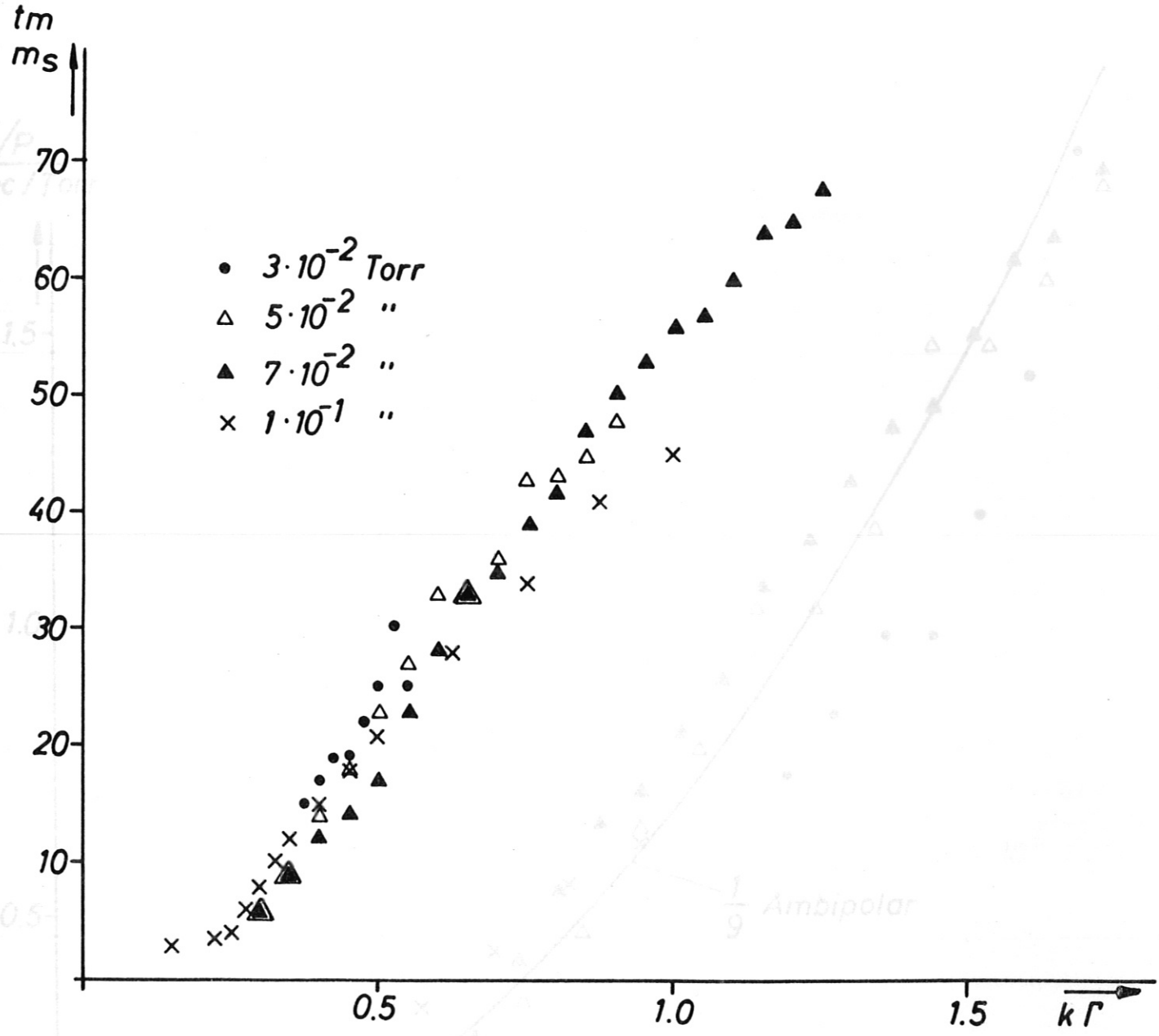

Fig. 5 The time t_m as a function of the magnetic field strength. r = 3.5 cm.

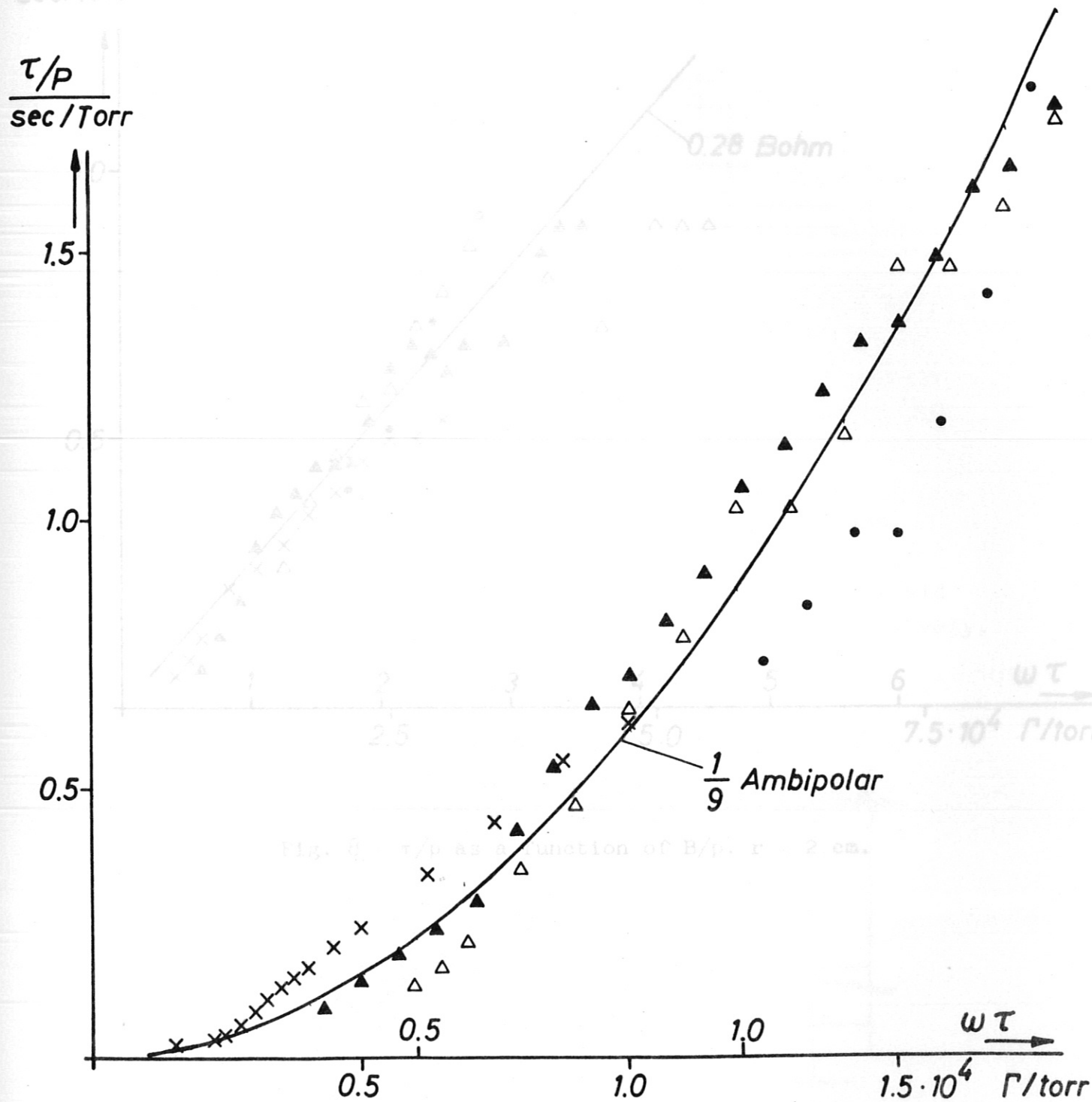

Fig. 6 τ/p as a function of B/p. r = 3.5 cm.

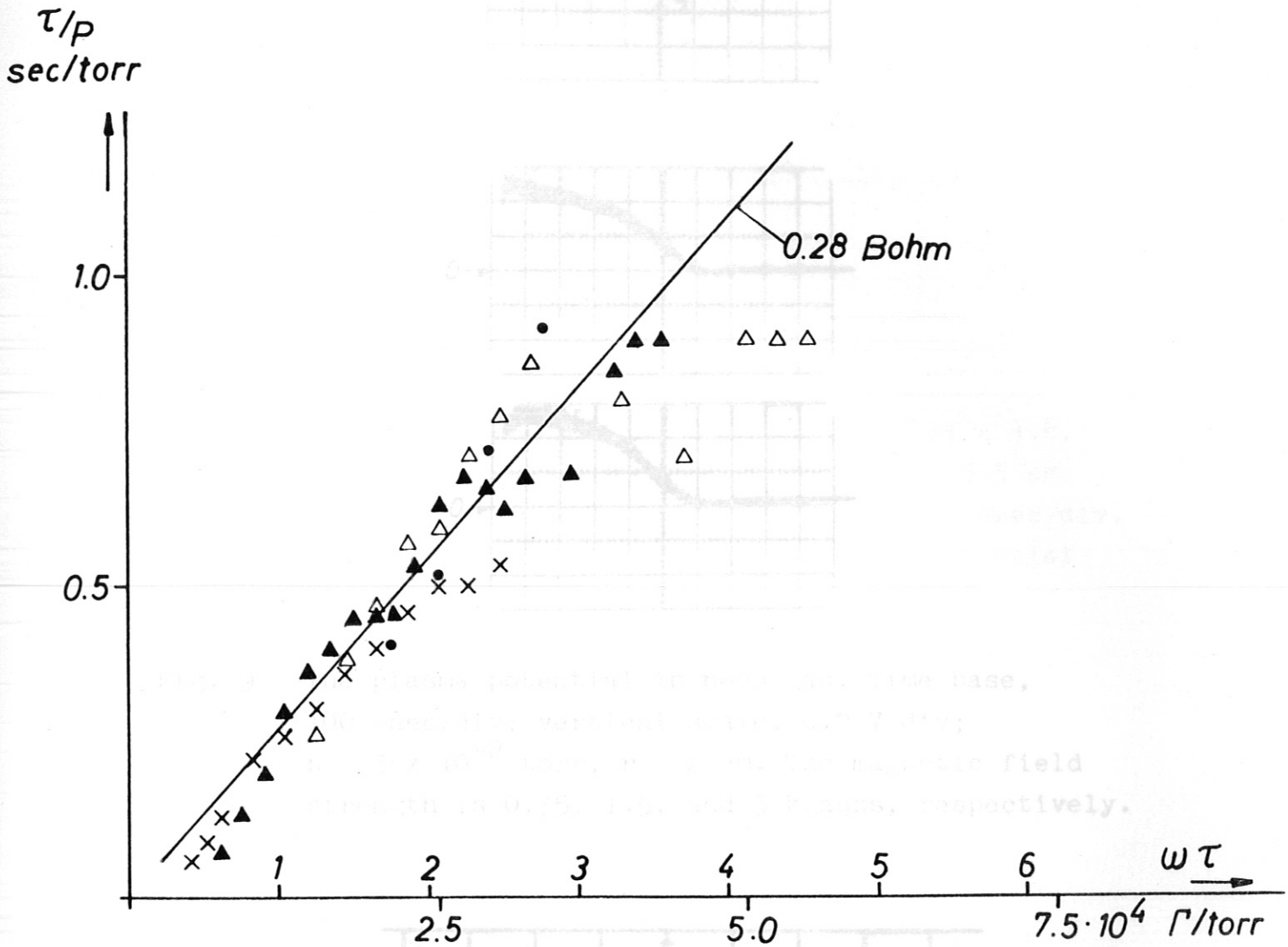

Fig. 8 τ/p as a function of B/p. r = 2 cm.

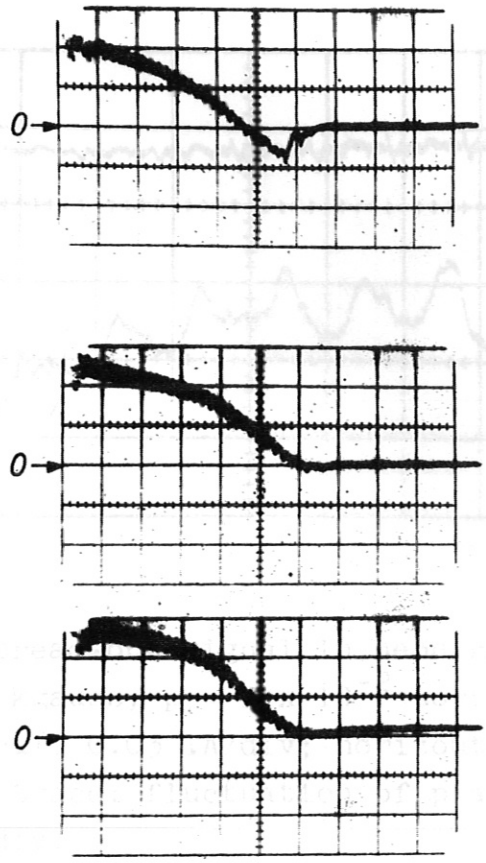

Fig. 9 The plasma potential in neon gas. Time base, 100 msec/div; vertical scale, 0.2 V/div; $p = 3 \times 10^{-2}$ torr, $r = 2$ cm. The magnetic field strength is 0.75, 1.5, and 3 kgauss, respectively.

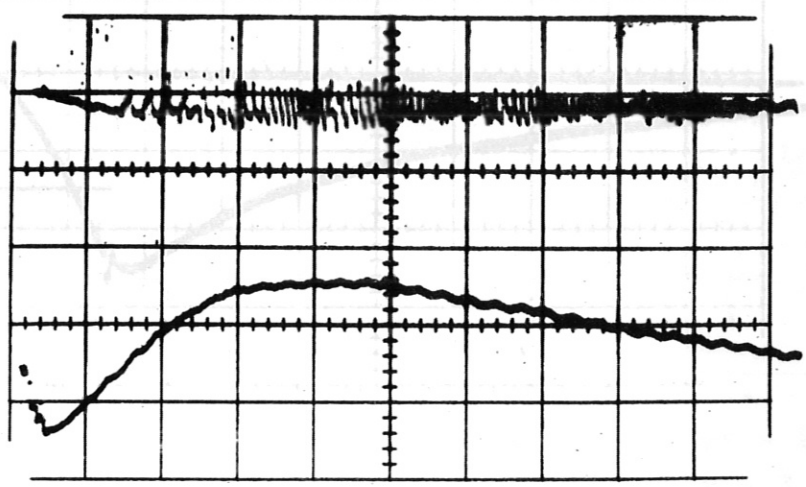

Fig. 10 The spread-out signal in neon gas. $\omega\tau = 0.35$, $B_o = 0.55$ kgauss, $p = 5 \times 10^{-2}$ torr, $r = 3.5$ cm. Vertical; 0.1 μA/div; horizontal 10 msec/div. Upper trace: fluctuation of plasma potential 2 mV/div.

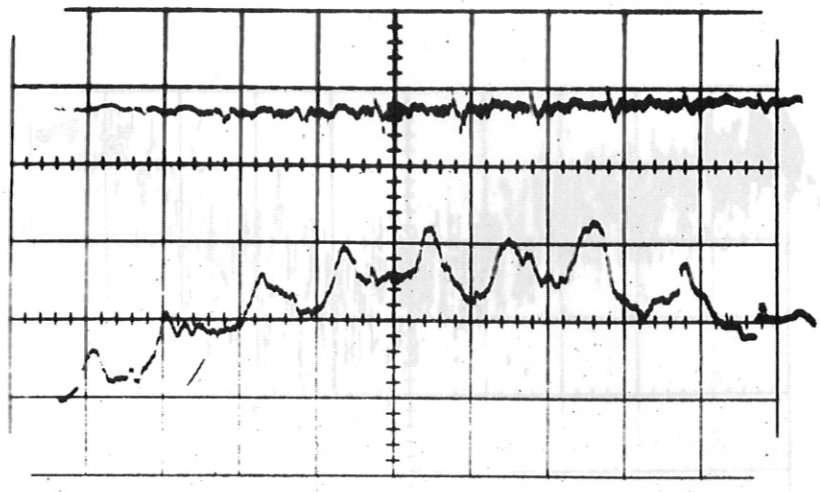

Fig. 11 The spread-out signal in neon gas. $\omega\tau = 4.8$, $B = 3$ kgauss, $p = 2 \times 10^{-2}$ torr, $r = 3.5$ cm. Vertical, 0.03 μA/div; horizontal, 20 msec/div. Upper trace: fluctuation of plasma potential 2 mV/div.

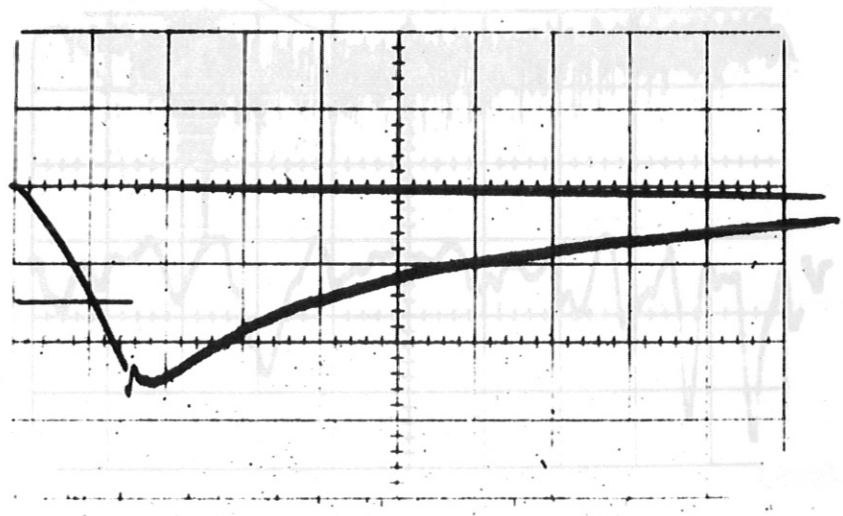

Fig. 12 The spread-out signal of electrons. $\omega\tau = 0.8$, $B_o = 0.5$ kgauss, $p = 5 \times 10^{-2}$ torr, $r = 2$ cm. Vertical, 3 μA/div; horizontal, 5 msec/div.

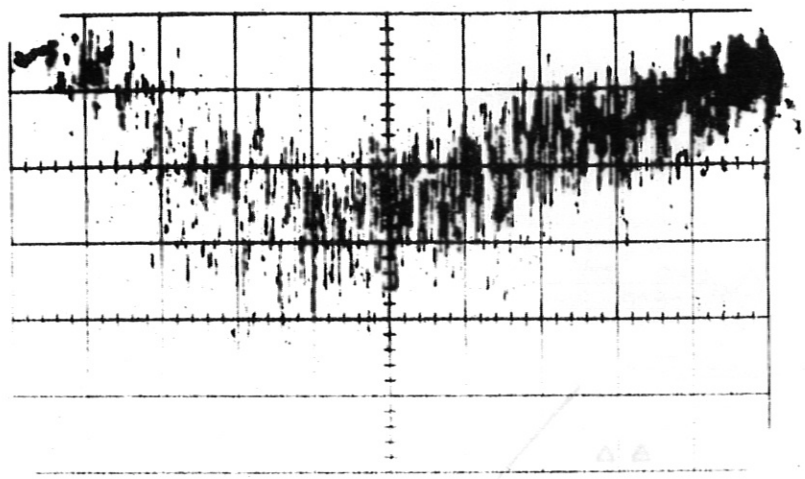

Fig. 13 The spread-out signal of electrons. $\omega\tau$ = 2.5, B_o = 1.5 kgauss, p = 5 x 10^{-2} torr, r = 3 cm. Vertical, 0.03 μA/div; horizontal 20 msec/div.

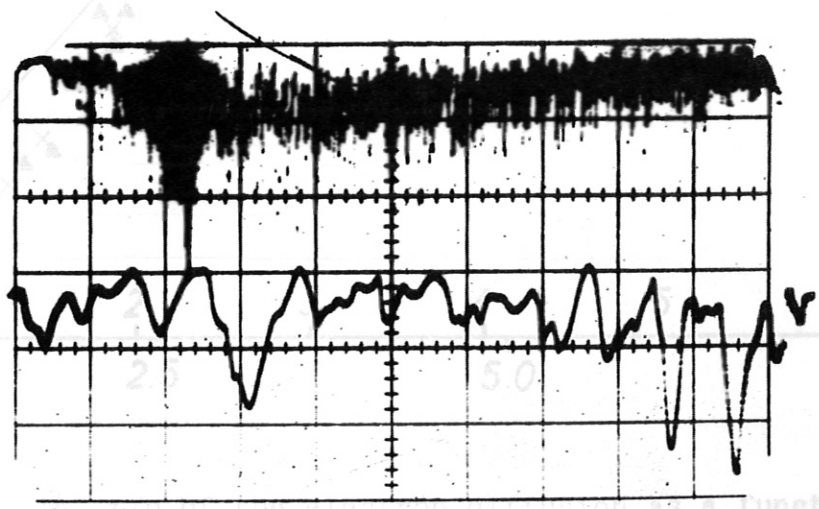

Fig. 13A The spread-out signal of electrons. $\omega\tau$ = 2.5, B_o = 1.5 kgauss, p = 5 x 10^{-2} torr, r = 3 cm. Upper trace: vertical, 0.1 μA/div; horizontal 20 msec/div;
Lower trace: vertical 0.1 μA/div; delay time 40 msec, horizontal, 0.5 msec/div.

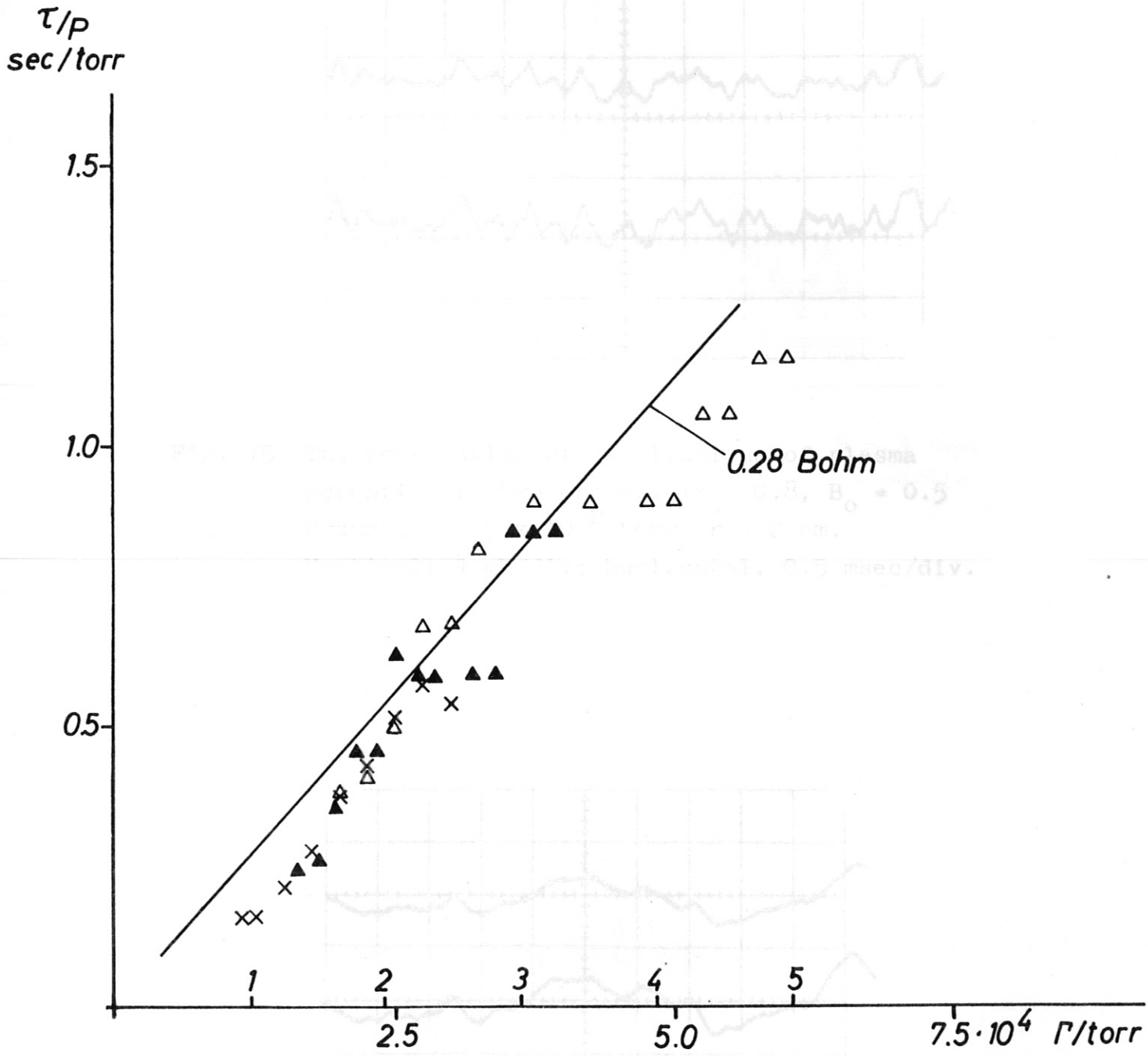

Fig. 14 τ/p of the electron diffusion as a function of B/p. r = 2 cm.

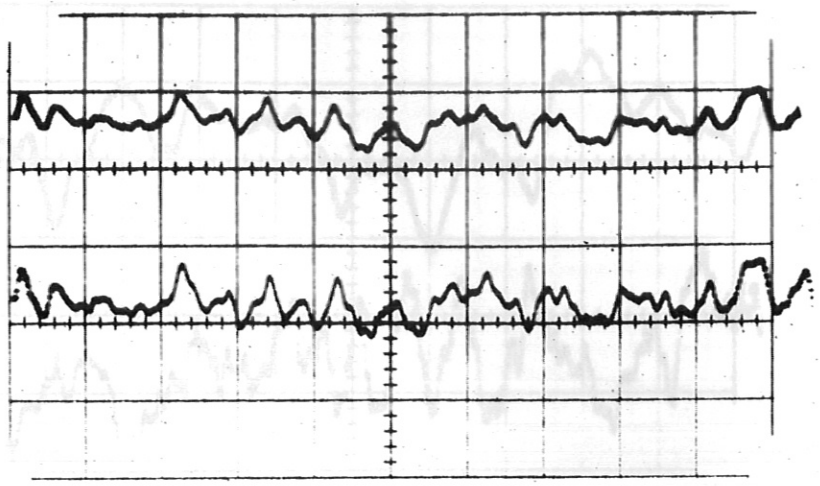

Fig. 15 The correlation of oscillations of plasma potential in two probes. $\omega\tau = 0.8$, $B_o = 0.5$ kgauss, $p = 5 \times 10^{-2}$ torr, $r = 2$ cm.
Vertical: 4 mV/div; horizontal, 0.5 msec/div.

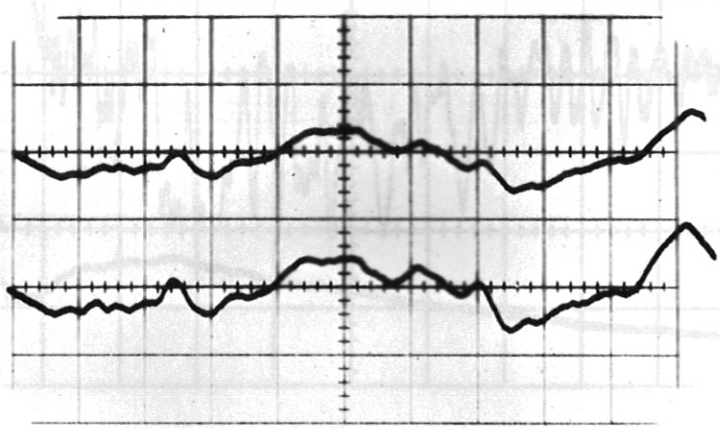

Fig. 16 The phase difference between oscillations in two probes. $\omega\tau = 0.8$, $B_o = 0.5$ kgauss, $p = 5 \times 10^{-2}$ torr, $r = 4$ cm.
Vertical, 2 mV/div; horizontal, 0.1 msec/div.

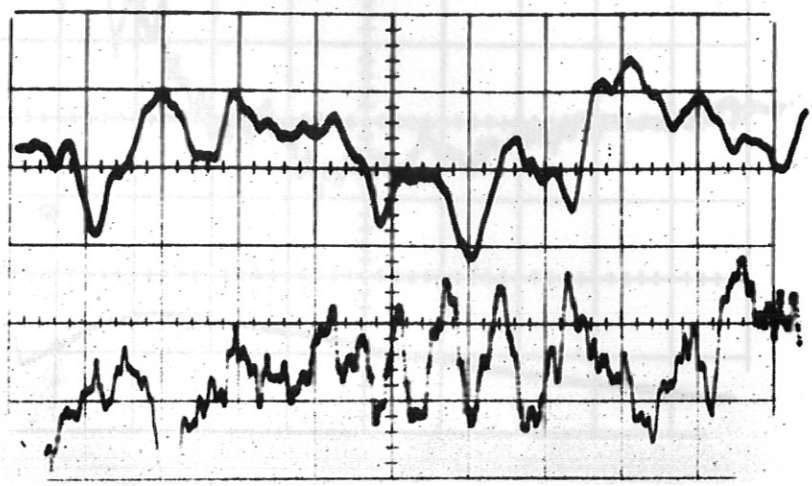

Fig. 17 Oscillations in two probes. $\omega\tau = 5.0$, $B_o = 3$ kgauss, $p = 5 \times 10^{-2}$ torr, $r = 2$ cm. Vertical, 2 mV/div; horizontal, 0.5 msec/div.

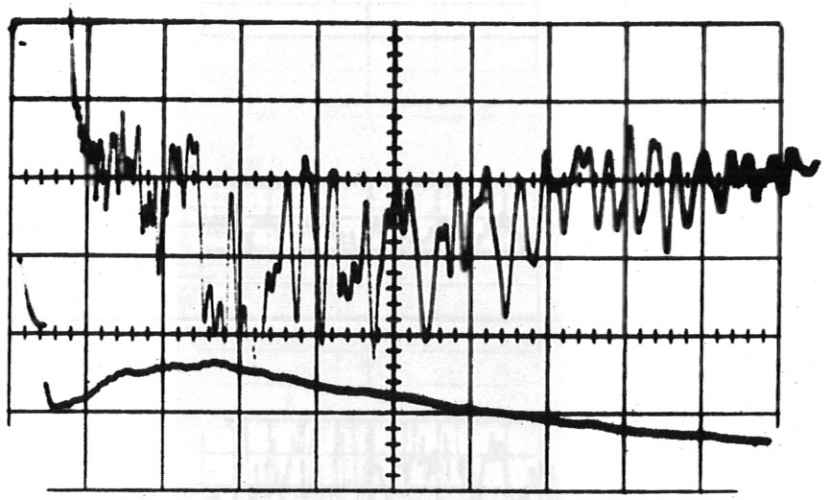

Fig. 18 The fluctuating electric field perpendicular to the magnetic field.
$\omega\tau = 1.2$, $B_o = 0.38$ kgauss, $p = 2.5 \times 10^{-2}$ torr, $r = 4$ cm. Vertical, 2mV/div; horizontal, 5 msec/div.

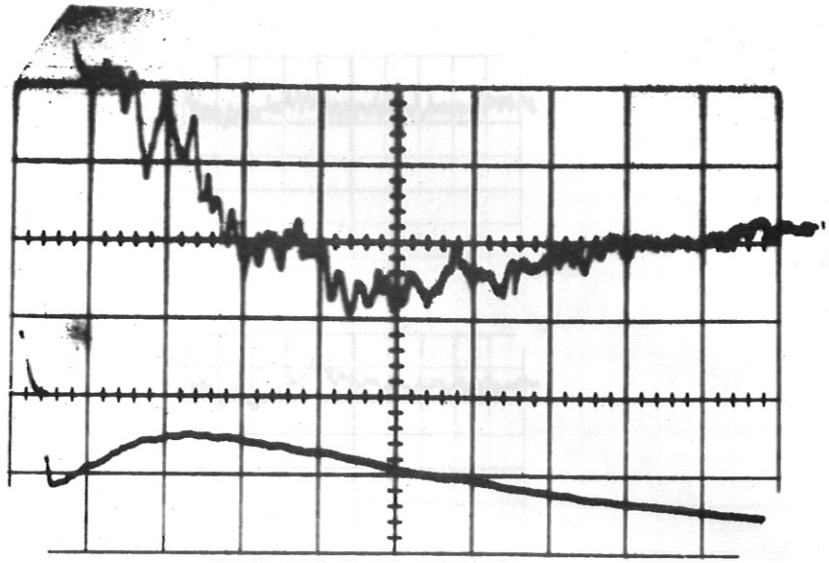

Fig. 19 The fluctuating electric field parallel to the magnetic field.
$\omega\tau$ = 1.2, B_o = 0.38 kgauss, p = 2.5 x 10^{-2} torr,
r = 4 cm. Vertical, 2 mV/div; horizontal, 5 msec/div.

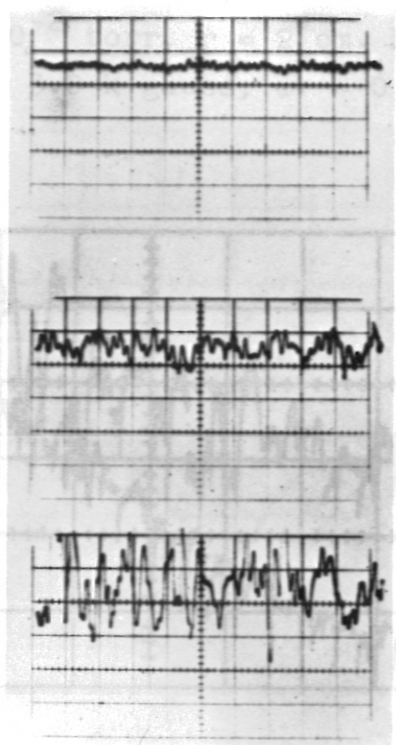

Fig. 20 The oscillations in the fluctuating electric field.
Time base 2 msec/div; vertical gain 2 mV/div,
p = 5 x 10^{-2} torr, r = 2 cm.
From top to bottom 0.5, 1.5, 3.0 kgauss,
$\omega\tau$ = 0.8, 2.4, 4.8.

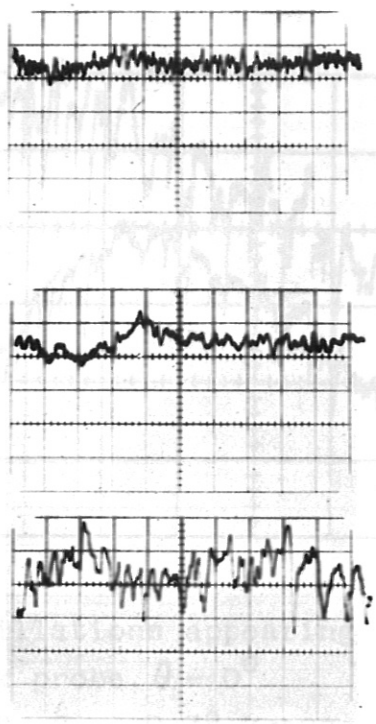

Fig. 21 The oscillations in the plasma potential. Time base 2 msec/div, vertical gain 4 mV/div, $p = 5 \times 10^{-2}$ torr, $r = 2$ cm. From top to bottom 0.5, 1.5, 3.0 k gauss, $\omega\tau = 0.8, 2.4, 4.8$.

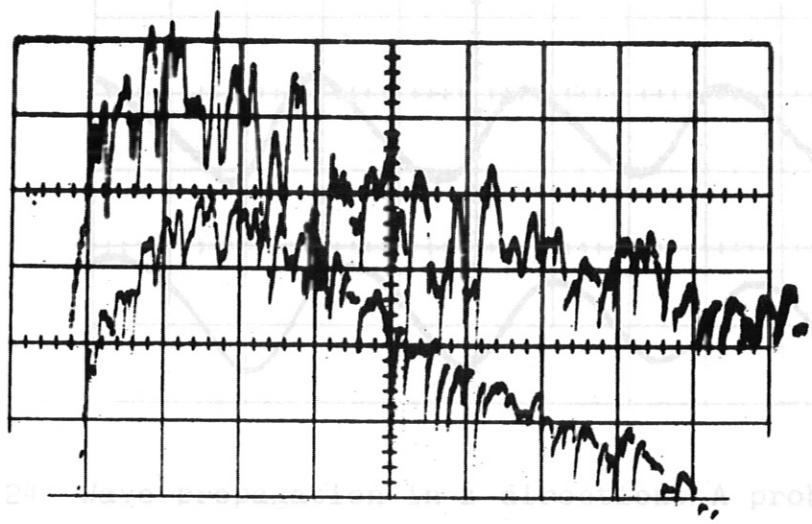

Fig. 22 The oscillations appearing in each branch of the fork probe. $\theta = 90^{\circ}$ $\omega\tau = 1.2$, $B_o = 0.38$ kgauss, $p = 2.5 \times 10^{-2}$ torr, $r = 4$ cm, vertical, 2 mV/div; horizontal, 5 msec/div.

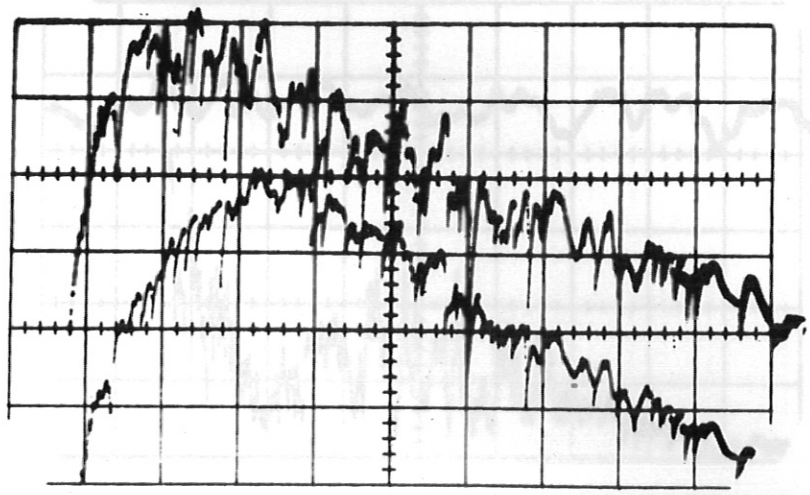

Fig. 23 The oscillations appearing in each branch of the fork probe. $\theta = 0^{o}$
$\omega\tau = 1.2$, $B_o = 0.38$ kgauss, $p = 2.5 \times 10^{-2}$ torr, $r = 4$ cm, vertical, 2 mV/div, horizontal, 5 msec/div.

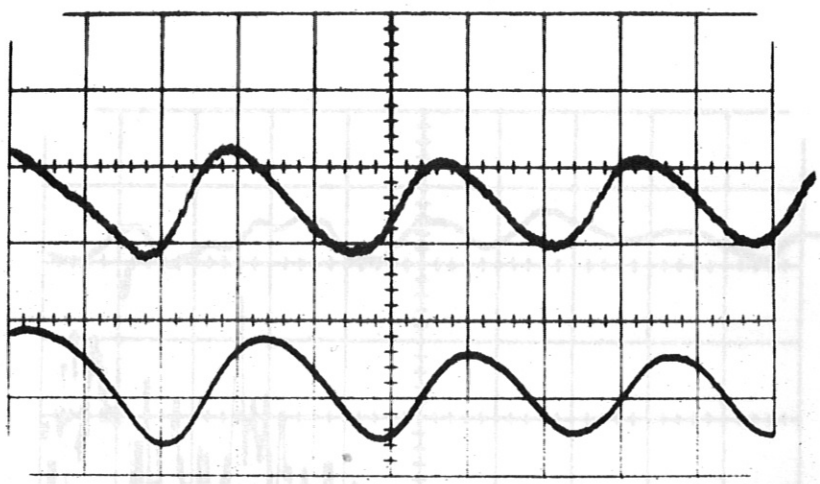

Fig. 24 Wave propagation in z-direction. A probe is located at the midplane of the apparatus and the other is located at the axial end of the chamber. $p = 5 \times 10^{-2}$ torr, $B_o = 1.25$ kgauss, $\omega\tau = 2$. Vertical, upper trace (end probe) 2 mV/div., lower trace 4 mV/div; horizontal, 0.2 msec/div.

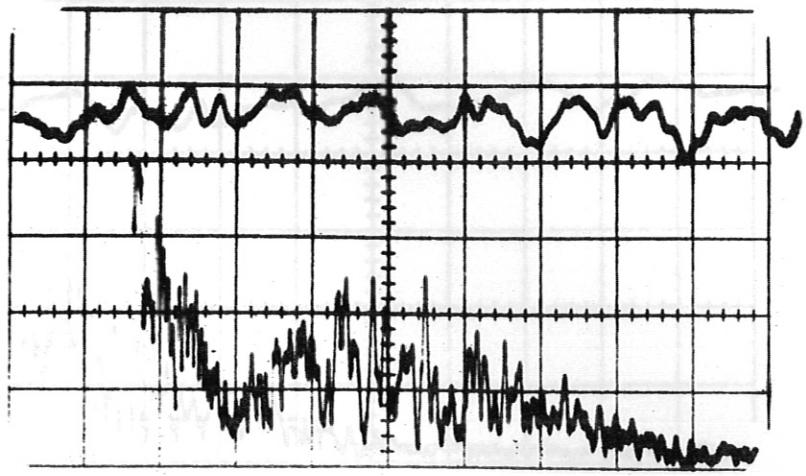

Fig. 25 The frequency spectrum of the fluctuation of plasma potential.
$\omega\tau = 0.8$, $B_o = 0.5$ kgauss, $p = 5 \times 10^{-2}$ torr.
Central frequency, 2 kHz; dispersion 500 Hz/div; vertical gain 10 mV/div. The upper trace is the fluctuation of floating potential.
Vertical 4 mV/div; horizontal 0.5 msec/div.

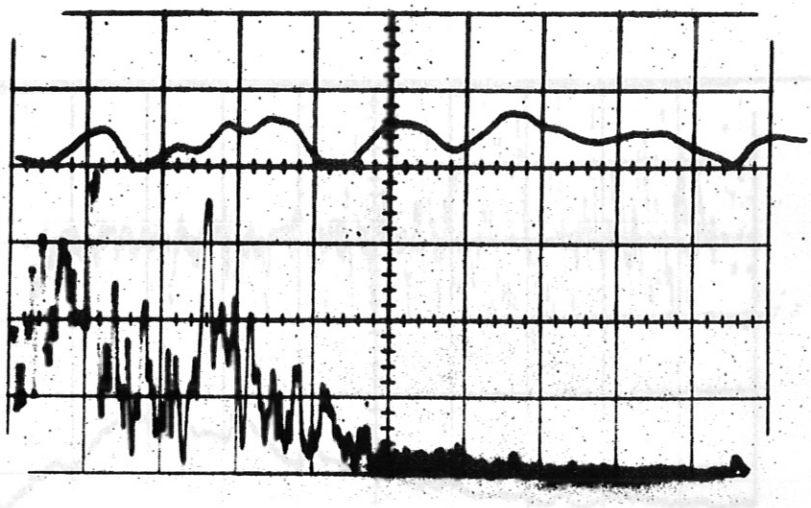

Fig. 26 The frequency spectrum in a stronger magnetic field.
Central frequency, 2 kHz; dispersion, 500 Hz/div; vertical gain 50 mV/div; $p = 5 \times 10^{-2}$ torr.
$B_o = 2$ kgauss; $\omega\tau = 3.3$. The upper trace is the fluctuations of floating potential. Vertical, 10 mV/div; horizontal 0.5 msec/div.

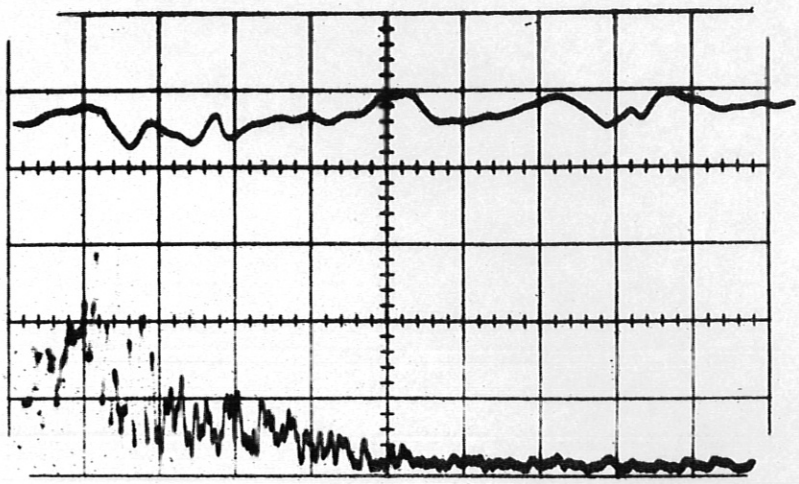

Fig. 27 The frequency spectrum in a stronger magnetic field.
Central frequency, 2 kHz; dispersion, 500 Hz/div; vertical gain 50 mV/div; $p = 5 \times 10^{-2}$ torr; B_o = 3 kgauss; $\omega\tau = 5$.
The upper trace is the fluctuations of floating potential. Vertical, 10 mV/div; horizontal, 0.5 msec/div.

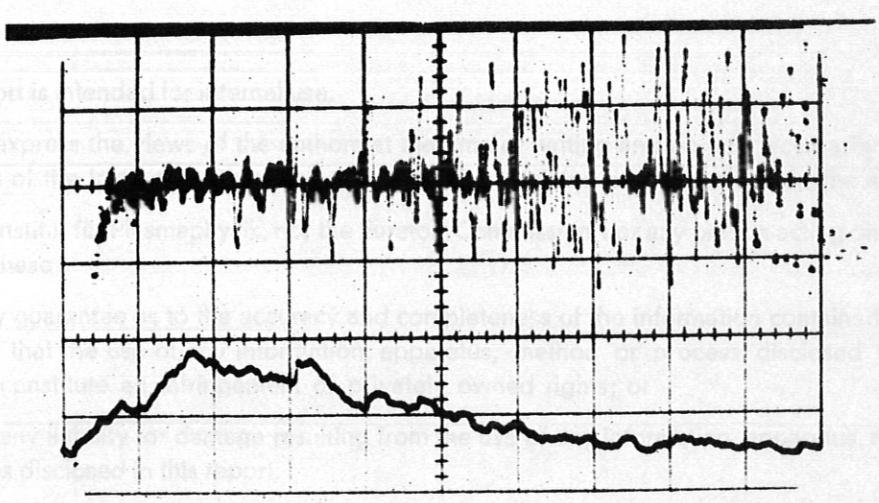

Fig. 28 Sometimes the oscillation amplitude grows during plasma decay.
$\omega\tau = 4.1$; B_o =1kgauss; $p = 2 \times 10^{-2}$ torr.
Vertical, 10 mV/div; horizontal, 5 msec/div;
Lower trace, spread-out signal.